LOCAL LOSS COEFFICIENT IN SUDDEN EXPANSION LAMINAR FLOWS OF INELASTIC SHEAR-THINNING FLUIDS

J. P. Miranda
Instituto Politécnico de Bragança, Escola Superior de Tecnologia e Gestão, Campus de Santa Apolónia, 5301-857 Bragança, Portugal
jmiranda@ipb.pt

F. T. Pinho
Centro de Estudos de Fenómenos de Transporte, DEMEGI, Faculdade de Engenharia, Universidade do Porto, Rua Dr. Roberto Frias s/n, 4200-465 Porto, Portugal
fpinho@fe.up.pt

P. J. Oliveira
Departamento de Engenharia Electromecânica, Universidade da Beira Interior, Rua Marquês D'Ávila e Bolama, 6201-001 Covilhã, Portugal
pjpo@ubi.pt

Abstract A numerical investigation was carried out to quantify the local loss coefficient in the laminar flow of shear-thinning inelastic fluids through an axisymmetric sudden expansion having a diameter ratio of 1 to 2.6. The finite-volume code used collocated meshes and second order interpolation schemes to discretize the diffusion and convective terms of the momentum equation. The investigation concentrated on quantifying the effects of shear-thinning (n) and Reynolds number (Re) on the local loss coefficient C_I. At low Reynolds numbers C_I varied inversely with Re, but tended to an asymptotic value at large values of Re. Regarding the effect of n, C_I raised by more than 100% when n decreased from 1.0 to 0.2 at low Re, whereas the asymptotic value of C_I decreased by more than 50%. However, this feature was shown to be related to the definition of the Reynolds number.

Keywords. Sudden expansion, pressure loss, shear-thinning fluid, laminar flow, inelastic fluid

1. Introduction

Sudden expansion flows occur frequently in many industrial applications and they have been extensively investigated in the past for Newtonian fluids both numerically (Habib and Whitelaw, 1982; Oliveira and Pinho, 1997) and experimentally (Stieglmeier *et al*, 1989; Back and Roshke, 1972) amongst others, in the laminar and mainly in the turbulent flow regimes.

When the fluids exhibit non-Newtonian characteristics the literature is scarcer. In the laminar flow regime we emphasize the works of Halmos and Boger (1975, 1976) and Halmos et al (1975) whereas in the turbulent regime experimental investigations have been carried out by Pak et al (1990, 1991), Castro and Pinho (1995), Escudier and Smith (1999) and Pereira and Pinho (2000, 2002). Other research on sudden expansion flows at very low Reynolds numbers concentrated on viscoelastic effects such as the works of Baloch et al (1995, 1996) and Missirlis *et al* (1998).

In spite of these efforts not much attention has been devoted to the issue of pressure losses in sudden expansions in a useful and practical way, hence Newtonian correlations are usually used to quantify the local loss coefficient. The exceptions were the experiments of Edwards et al (1985) and the theoretical work of Gupta (1965). The main objective of Edwards et al (1985) was to experimentally find the variation of the irreversible pressure loss coefficient with the Reynolds number for Newtonian and power law fluids. At low Reynolds numbers they reported the inverse law ($C_I = A / Re$) with a coefficient A that depended on the expansion ratio but not on the power law index. At intermediate Reynolds numbers ($Re \approx 250$), C_I varied linearly with Re and then it tended to an asymptotic value regardless of fluid rheology. Unfortunately, by not accounting for the differences between the true and fully-developed friction losses in the upstream and downstream pipes, their coefficients are not correct.

The recent investigations of Oliveira and Pinho (1997) and Oliveira et al (1998) for laminar Newtonian flows have clearly demonstrated that the local loss coefficient differs by a large amount from the standard expressions found in reference books and manuals, with the differences increasing as the Reynolds number is reduced. These differences are bound to be more severe with non-Newtonian fluids and this work is aimed at quantifying them numerically in a systematic way for inelastic shear-thinning fluids, and also at reporting other hydrodynamic characteristics of the flow in axisymmetric sudden expansions

The next section presents the problem and the numerical method, then a one-dimensional theory that helps explain the various contributions to C_I is briefly outlined and the results are presented in Section 4.

2. Basic equations and the numerical method

Figure (1) shows schematically the axisymmetric sudden expansion and the computational domain used. There is a long pipe of length L_1 and diameter D_1 upstream of the sudden expansion to ensure a fully-developed inlet flow. Downstream of the sudden expansion plane the pipe is also sufficiently long (length L_2, diameter D_2) for the flow to redevelop again. The expansion investigated had a diameter ratio of 1:2.6.
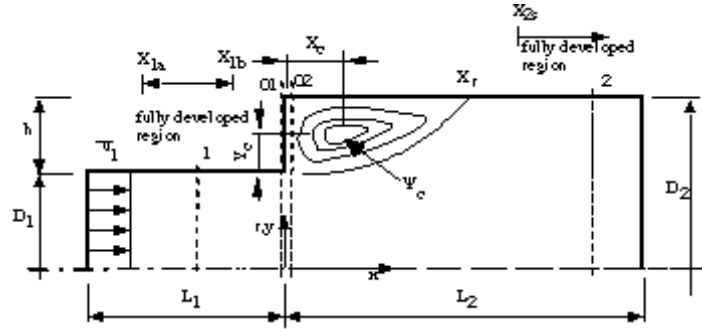

Figure 1. Schematic representation of sudden expansion geometry and control volume.

The calculations are aimed at obtaining various global flow characteristics such as the normalized recirculation length ($X_R \equiv x_r/h$, $h = (D_2 - D_1)/2$), the maximum value of the stream function in the recirculation region (ψ_{max}) and the local loss pressure coefficient C_I ($C_I \equiv (\Delta p - \Delta p_R - \Delta p_F)/\frac{1}{2}\rho\overline{u_1}^2$, where subscripts R and F denote "reversible" and "fully-developed" pressure drops. To this aim it is necessary to solve numerically the continuity equation (Eq. 1) and the momentum equation (Eq. 2), where the rheological constitutive equation is that of a purely viscous Generalized Newtonian fluid with the viscous function $\eta(\dot\gamma)$ represented by the power law model (Eq. (3)). The shear rate $\dot\gamma$ is related to the second invariant of the rate of deformation tensor (D_{ij}) in Eq. (4).

$$\frac{\partial u_i}{\partial x_i} = 0 \tag{1}$$

$$\rho\left[\frac{\partial u_i}{\partial t} + \frac{\partial(u_i u_j)}{\partial x_j}\right] = -\frac{\partial p}{\partial x_i} + \frac{\partial}{\partial x_j}\left[\eta(\dot\gamma)\left(\frac{\partial u_i}{\partial x_j} + \frac{\partial u_j}{\partial x_i}\right)\right] \tag{2}$$

$$\eta(\dot\gamma) = k\dot\gamma^{n-1} \tag{3}$$

$$\dot\gamma = \sqrt{2D_{ij}D_{ij}} \text{ with } D_{ij} = \frac{1}{2}\left(\frac{\partial u_i}{\partial x_j} + \frac{\partial u_j}{\partial x_i}\right) \tag{4}$$

Equations (1) and (2) were solved with a general-purpose finite-volume CFD code, developed by Oliveira (1992), for non-staggered meshes. Extension to deal with inelastic non-Newtonian fluids of variable viscosity is straightforward. The discretization and interpolation schemes adopted were all second order: central differences (CDS) for diffusion and second order upwind (SOU) for convection. Pressure-velocity coupling was dealt with Rhie-and-Chow's method and the computing algorithm adopted was a time-marching form of the SIMPLEC algorithm developed by Issa and Oliveira (1994). The sets of linear equations were solved with conjugate gradient methods (preconditioned biconjugate solver for u and v, symmetric conjugate solver for p), and all the calculations were performed with a Pentium/133 MHz computer with 128 Mb RAM.

The solution of a 2D axisymmetric flow problem with a 3D code for non-orthogonal coordinates and Cartesian velocity components requires the use of a computational domain in the form of a triangular wedge to represent a sector of a circular cross-section. This is current practice but requires a modified bulk velocity in the calculations (U) so that the mass flow rate is identical to that in a circular pipe with bulk velocity V and the friction factor must be calculated by

$$f = \frac{4\tau_w}{\frac{1}{2}\rho U^2}\frac{D}{2Y} \tag{5}$$

where D is the pipe diameter and Y is the height of the triangular cross-section.

3. Approximate one-dimensional theory

The main quantity of interest in this work is the irreversible pressure loss coefficient (C_I) which is defined as

$$C_I \equiv \frac{\Delta p_I}{\frac{1}{2}\rho U_1^2} \tag{6}$$

where the overall pressure drop between planes 1 and 2 in Fig. (1) ($\Delta p = p_1 - p_2$) has been decomposed into irreversible (*I*), reversible (*R*) and fully-developed (*F*) pressure drops: $\Delta p = \Delta p_I + \Delta p_R + \Delta p_F$. The irreversible pressure drop Δp_I includes not only the effect of the sudden expansion itself but also a friction effect, because the actual friction loss between planes 1 and 2 (c.f. Fig. (1)) is different from the corresponding fully developed friction loss. In this work, the approximate one-dimensional theory underlying the calculation of the loss coefficient for Newtonian fluids presented by Oliveira and Pinho (1997) is adopted. For purely viscous fluids the theory is independent of the fluid viscosity law except for the profile shape factors for energy $\alpha \equiv \overline{u^3}/\overline{u}^3$ and momentum $\beta \equiv \overline{u^2}/\overline{u}^2$, where the overbar denotes average over the cross-section of the pipes. For power law fluids with power index *n* in fully-developed flow those two factors are given by

$$\alpha = \frac{3(3n+1)^2}{(2n+1)(5n+3)} \quad \text{and} \quad \beta = \frac{3n+1}{2n+1} \tag{7}$$

Oliveira and Pinho (1997) have demonstrated that the true pressure loss for Newtonian fluids differed significantly from the standard theory coefficient (C_{I-th}) found in manuals and textbooks, and their theory explained the differences via Eq. (8).

$$C_{Ic-th} = C_{I-th} - \left\{ \Delta C_F + \Delta C_\beta - \Delta C_{p_o} \right\} \tag{8}$$

In Eq. (8) C_{Ic-th} is the corrected coefficient and the various corrective terms account for wall friction effects (*F*), variation of momentum shape factor (β), and non-uniform pressure at the expansion plane (p_0), respectively. The standard theoretical loss coefficient is given by

$$C_{I-th} = \alpha_1 \left(1 - \frac{\alpha_2}{\alpha_1}\sigma^2 \right) - 2\beta_1 \sigma \left(1 - \frac{\beta_2}{\beta_1}\sigma \right) \tag{9}$$

which can be further simplified for conditions of fully developed flow at inlet and outlet (σ is the area ratio, $A_1/A_2 \equiv (D_1/D_2)^2$) and for conditions of uniform velocity profile ($\alpha = \beta = 1$), this latter case leading to the well-known Borda-Carnot coefficient equal to $(1-\sigma)^2$. The first term on the right-hand-side of Eq. (9) is the "reversible" pressure recovery readily obtained from application of Bernoulli's equation.

4. Results and discussion

4.1. Uncertainties and validation of results

For power law fluids the Reynolds number used is the Generalized Reynolds number of Metzner and Reed (1955), here defined in terms of smaller pipe characteristics

$$\text{Re}_{gen} = \frac{\rho D_1^n U_1^{2-n}}{k} 8 \left(\frac{n}{6n+2} \right)^n \tag{10}$$

where subscript 1 refers to the inlet pipe and *k* and *n* are the consistency and power indices of the Ostwald de Waele power law (Eq. 3). The use of this Reynolds number is justified by the primary objective of this work since it facilitates the processing of the frictional loss in fully-developed pipe flow. However, the use of Re_{gen} can be misleading in terms of data interpretation, hence a second modified Reynolds number Re_{mod}, defined in Eq. (11), will also be used.

$$Re_{mod} = \frac{\rho D_1^n U_1^{2-n}}{k} \tag{11}$$

We start by presenting results that quantify numerical accuracy. For fully developed laminar flow in a straight pipe

the use of a uniform mesh with 20 radial cells resulted in values of the Darcy friction factor that differed from theoretical values by 0.31% for $n= 1$, 0.5% for $n= 0.4$ and 0.75% for $n= 0.2$. The increased error with shear-thinning is a consequence of the increased stiffness of matrices due to the very high viscosities in the centre of the pipe. The accuracy can be improved with mesh refinement but especially by using stricter convergence criteria (in all calculations reported here the stopping criteria was a normalized residual L_1 equal to 1×10^{-5}).

The corresponding predictions of the velocity profile are shown in Fig. (2) which plots radial profiles of the normalized axial velocity for different values of the power index and for a Reynolds number of 200. The agreement is as good as for the friction factor, again deteriorating with shear-thinning: the differences between the predicted and the theoretical velocity profile are within 0.2% for $n= 0.8$ and $n= 1.0$, 0.4% for $n= 0.4$ and $n= 0.6$ and increase to a value of the order of 1% for $n=0.2$.
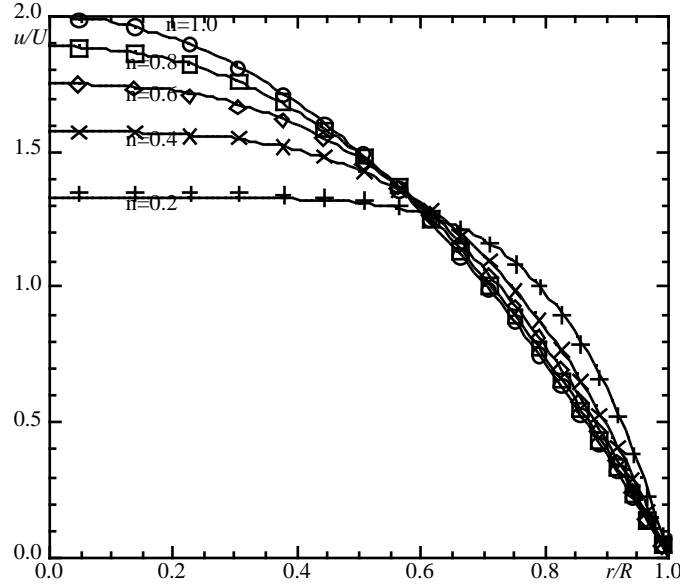

Figure 2. Radial profiles of the normalised axial velocity for power law fluids: symbols- calculations; lines: theory.

In the sudden expansion numerical calculations were carried out in three consecutively refined meshes and the effect of shear-thinning on numerical accuracy was also assessed. The mesh characteristics are those in Tab. (1) and mesh M2S is that used by Oliveira and Pinho (1997). The block-structured meshes are made of three blocks: block I in the inlet pipe, block II downstream of block I in the outlet pipe and block III downstream of the expansion wall. These meshes, designated by "Short" meshes, were used for simulations at low generalized Reynolds number flows ($Re_{gen} \leq 50$) and for fluids with high values of n ($n=0.4$ to 1.0); for $Re_{gen} > 50$ and $n= 0.2$, grids with longer inlet and outlet pipes had to be used ($L_1/D_1 = 100$, $L_2/D_2 = 100$). More details on these meshes can be found in Miranda (1999).

Table 1. Characteristics of the meshes for the standard geometry ($L_1/D_1= 20$, $L_2/D_2= 20$).

Mesh	Block I				Block II				Block III			
	N_x	N_y	f_x	f_y	N_x	N_y	f_x	f_y	N_x	N_y	f_x	f_y
M1S	20	10	0.7517	0.8530	35	10	1.1909	0.8530	35	16	1.1909	1.1025
M2S	40	20	0.8670	0.9236	70	20	1.0913	0.9236	70	32	1.0913	1.0500
M3S	80	40	0.9311	0.9610	140	40	1.0447	0.9610	140	64	1.0447	1.0247

With the predictions of the local loss coefficient C_I and of the normalized recirculation length X_R from these three meshes, "corrected" values of C_I and X_R were estimated using the technique of Richardson extrapolation to the limit (e.g. Ferziger, 1981). These quantities are listed in Tabs. (2) and (3) for $n= 1$ and $n= 0.4$, respectively and include also estimates of numerical uncertainty. The numerical uncertainties for any given quantity A, calculated in the medium mesh, were then estimated as $\varepsilon = (A_{M2} - A_{ext})/A_{ext} \times 100$, where the subscript ext indicates the extrapolated value and $M2$ refers to values obtained with mesh M2 (M2S or M2L, as appropriate).

The uncertainties in C_I are fairly constant with n, tending to increase for very low Reynolds numbers, and less so at high Reynolds numbers. In any case, uncertainties exceeding 1% are not expected at high Reynolds numbers but can go to 2% at low Reynolds numbers. For the normalized recirculation length and the eddy strength (Ψ_{max}) the deterioration in accuracy is more intense and errors can go up to about 10% at low Reynolds numbers and 5% at high Reynolds numbers with strongly shear-thinning fluids. As the main objective of this work was the determination of C_I, for which

mesh M2 is adequate to provide accurate results, this mesh was used throughout. Further comparisons with Newtonian and non-Newtonian fluids, to ascertain uncertainties and numerical accuracy, can be found in Oliveira and Pinho (1997) and Miranda (1999).

Table 2. Estimated numerical uncertainty in the calculation of C_I and X_R for fluids with n=1.

Re_{gl}	C_I					X_R				
	M1	M2	M3	$C_{I,ext}$	ε [%]	M1	M2	M3	$X_{R,ext}$	ε [%]
0.1	165.107	166.689	167.380	168.004	+0.78	0.4583	0.4799	0.4856	0.4876	-1.57
4	4.270	4.291	4.299	4.305	-0.33	0.6682	0.6815	0.6856	0.6871	-0.82
60	1.305	1.307	1.309	1.311	-0.36	6.141	6.114	6.104	6.100	+0.23

Table 3. Estimated numerical uncertainty in the calculation of C_I and X_R for fluids with n=0.4.

Re_{gl}	C_I					X_R				
	M1	M2	M3	$C_{I,ext}$	ε [%]	M1	M2	M3	$X_{R,ext}$	ε [%]
0.1	288.785	286.771	285.254	283.397	+1.19	0.1331	0.1517	0.1595	0.1663	-8.78
4	7.355	7.160	7.127	7.137	+0.32	0.1671	0.1758	0.1858	0.1996	-11.9
60	0.904	0.904	0.901	0.896	+0.89	1.658	1.667	1.685	1.712	-2.62

4.2. Eddy length and strength

Results of the normalized recirculation length $X_R \equiv x_r/h$ and of the eddy strength Ψ_{max} as a function of the shear-thinning intensity and Reynolds number are shown in Figs. (3) and (4), respectively. For Newtonian fluids, calculations of the eddy length and strength compare well with results from the literature (Oliveira and Pinho (1997); Macagno and Hung (1967); Badekas and Knight (1992) and Scott et al (1986) amongst others). At very low Reynolds numbers the calculated value of X_R of around 0.47 agrees well with the results reported in the literature and here it is important to notice that for creeping flow conditions the flow around a sudden contraction is identical to that around a sudden expansion. For a 1:2 sudden expansion Macagno and Hung (1967) calculated $X_R = 0.54$ and for a 1:2.26 expansion Monnet et al (1982) measured $X_R = 0.476$. For sudden contractions Nguyen and Boger (1979) found a constant x_r/D_2 between 0.17 and 0.18 for diameter ratios above than 4. Subsequent work (for instance Coates et al, 1992) has confirmed $x_r/D_2 = 0.17$ which is equivalent to $X_R = 0.46$ for a 1:4 expansion.
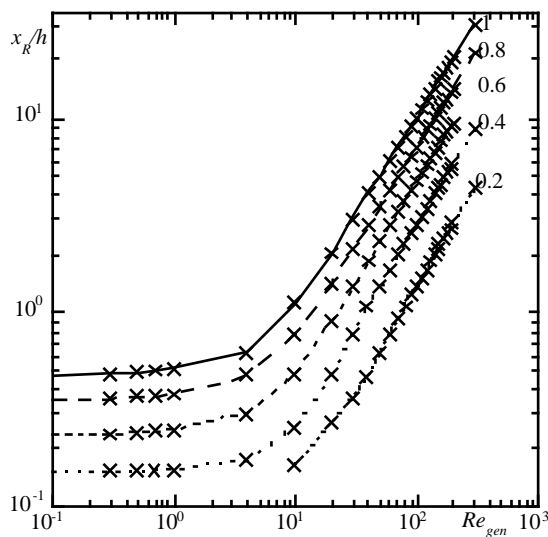

Figure 3. Variation of X_R with n and Re_{gen} in a 1:2.6 sudden expansion.
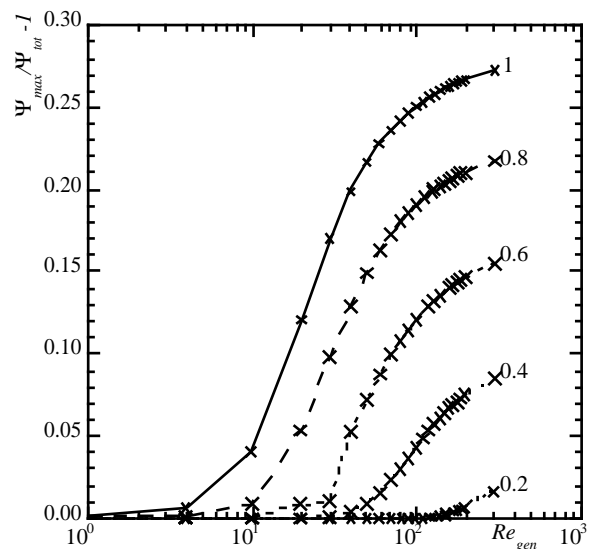
Figure 4. Variation of $\Psi_{max}/\Psi_{tot} - 1$ with n and Re_{gen} in a 1:2.6 sudden expansion.

For $n= 0.2$, X_R also asymptotes to a constant value at low Reynolds number, but these data are not shown in the figure due to their lower accuracy, for the reasons explained in Section 4.1.

The intensity of the recirculation bubble Ψ_{max} shown in Fig. (4) was determined from the predicted stream functions field Ψ. The stream function was calculated from an integration of the local flow rate starting at the pipe

axis. The figure shows how the eddy strength decreases with increased shear-thinning, because the local viscosity inside the recirculating region tends to increase due to the low shear rates there. This has also been observed in contour plots of the viscosity, which are not shown here for reasons of space. This increased viscosity within the recirculation region is also responsible for the reduction in its length seen in Fig. (3). Nevertheless, notice that at low Reynolds numbers the eddy has a small but finite recirculation intensity.

4.3. Local loss coefficient

The variation of the local loss coefficient with shear-thinning intensity and the Reynolds number is plotted in Fig. (5); in Fig. (5-a) the generalized Reynolds number Re_{gen} is used whereas Re_{mod} is the independent parameter in Fig. (5-b). As with the Newtonian fluid results of Oliveira and Pinho (1997), two regions of behaviour are observed: at high Reynolds numbers ($Re_{gen} > 50$) C_I tends to a constant value, as is typical of an inertia dominated flow behaviour, whereas at low Reynolds numbers the flow field is totally dominated by viscous effects and C_I varies as $1/Re$.

When the generalised Reynolds number is adopted (Fig. (5-a)), the effect of shear-thinning appears to act in opposition at the two Reynolds number ranges: at high Reynolds numbers the loss coefficient decreases with shear-thinning, whereas at low Reynolds numbers shear-thinning increases the pressure loss. It should be clear, however, that the trends of the C_I variation with Re seen in Fig. (5-a) are, to a large extent, influenced by the definition adopted for the Reynolds number. In fact, if the same C_I data are plotted in Fig. (5-b) as a function of the modified Reynolds number (Eq. 11) then, a reduction of the local loss coefficient with shear-thinning is observed throughout the whole range of Reynolds numbers. At low Reynolds numbers, use of the Re_{gen} gives rise to the misleading trends seen in Fig. (5-a) and for that reason it is better to consider Re_{mod} as the main independent parameter for the physical characterisation of pressure losses in the expansion. However, Re_{gen} will still be employed for the correlation developed in Section 4.4 below, because it facilitates calculation of pressure losses in piping systems, which are historically based on the notion of a generalised Reynolds number giving the same friction factor as for a Newtonian fluid in a straight pipe (that is, $f = 64/Re_{gen}$)
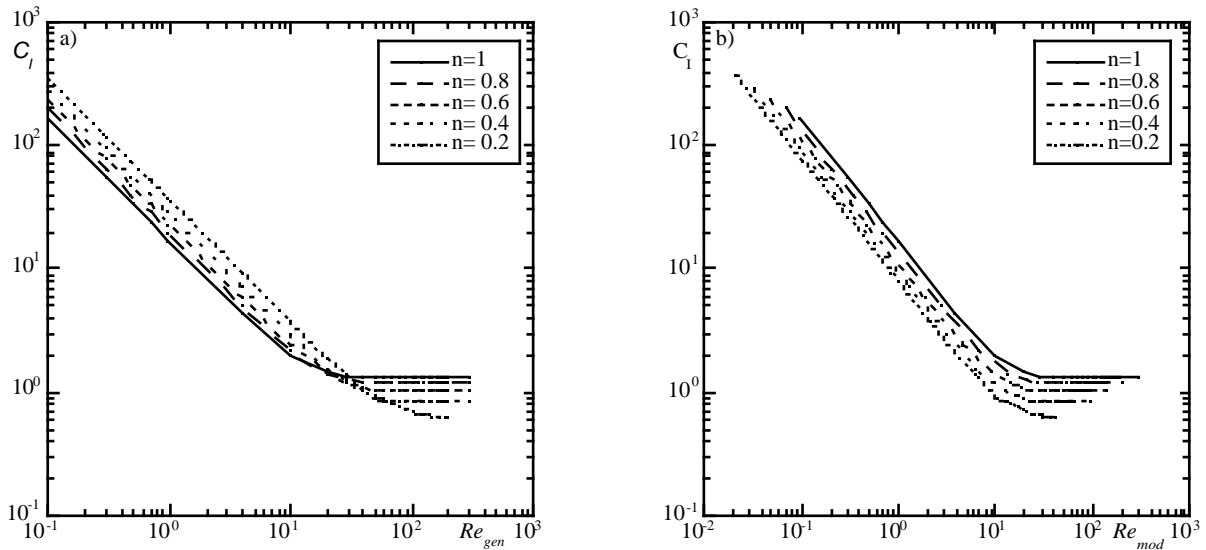

Figure 5. Variation of C_I with n and Reynolds number in a sudden expansion with 1:2.6: (a) as a function of the generalized Reynolds number, Eq. (10); b) as a function of the modified Reynolds number, Eq. (11).

The computed values of C_I for power law fluids differ significantly from the values usually quoted in the literature C_{I-th} and this discrepancy increases with shear-thinning: at high Reynolds number, where the "standard" value is numerically and physically more correct, C_{I-th} differs from the true value C_I by 24% for a Newtonian fluid, the difference growing to 37% for $n= 0.6$ and 64% for $n= 0.2$. One would think more logical the opposite trend because the velocity profiles flatten with shear-thinning, thus approaching the condition used to derive C_{I-th}. However, the viscous effects associated with n far outweigh the effect of the velocity profile shape. It is possible to partially correct the "standard" value and Tables (4) and (5) lists such corrections (C_{Ic-th}, Eq. (8)) for $n= 0.8$ and 0.6. For other values of n see Miranda (1999).

The approximate one-dimensional theory easily explains the discrepancies between values of C_I and those commonly found in the literature (C_{I-th}), but does not provide the exact equations to transform C_{I-th} into C_{Ic-th}. The theory works pretty well for $n \geq 0.6$, whereas for more shear-thinning fluids the errors exceed 5%, especially at low

Reynolds numbers (for instance, 9% and 17% for $n= 0.4$ and 0.2, respectively). This loss of accuracy is not due to a lack of mesh refinement but to the need for tighter convergence criteria than the L_I-norm value of 1×10^{-5} used here when fluids are strongly shear-thinning. Such highly shear-thinning fluids develop very high viscosities within the recirculating regions which increase the stiffness of matrices (Pinho, 2001). This would again increase the computing time by a significant amount and was not done because it was unlikely to have a significant effect on the calculated value of C_I: the local loss coefficient was obtained from the pressure variation along the centreline, whereas the stiff matrices tend to concentrate more in the recirculating region and so will have more impact on the corrective terms ΔC_{p0} and ΔC_{F2}.

Table 4. Predicted (C_I), corrections and corrected theoretical loss coefficient (C_{I-th}) in the 1:2.6 sudden expansion for n=0.8. C_{Ic-th} = 1.534.

Re_{gen}	C_I	β_{01}	ΔC_β	ΔC_{F1}	ΔC_{F2}	ΔC_{p0}	C_{Ic-th} (Eq 8)	*$Error$ [%]
0.0987	196.7	1.197	0.1886	-26.75	20.10	167.3	175.3	- 10.9
0.4933	39.34	1.199	0.1852	-5.324	4.067	36.49	39.10	- 0.6
0.9865	19.76	1.202	0.1807	-2.623	2.065	17.65	19.56	- 1.0
3.946	5.012	1.215	0.1579	-0.6098	0.5732	3.564	4.976	- 0.7
19.73	1.435	1.255	0.0898	-0.0892	0.2578	0.1645	1.440	+ 0.3
49.33	1.201	1.278	0.0506	-0.0253	0.2766	-0.0275	1.205	+ 0.3
98.66	1.184	1.289	0.0318	-0.0096	0.2930	-0.0334	1.185	+ 0.1
148.0	1.188	1.294	0.0233	-0.0054	0.2995	-0.0275	1.189	+ 0.1
197.3	1.192	1.296	0.0199	-0.0036	0.3029	-0.0229	1.191	- 0.02

$* \ Error = \left(C_{Ic-th} - C_I\right)/C_I \times 100$

Table 5. Predicted (C_I), corrections and corrected theoretical loss coefficient (C_{I-th}) in the 1:2.6 sudden expansion for n=0.6. C_{Ic-th} = 1.422.

Re_{gen}	C_I	β_{01}	ΔC_β	ΔC_{F1}	ΔC_{F2}	ΔC_{p0}	C_{Ic-th} (Eq 8)	*$Error$ [%]
0.0984	235.2	1.170	0.1750	-26.71	34.73	231.4	224.6	- 4.5
0.4921	46.90	1.171	0.1716	-5.278	6.996	45.39	44.92	- 4.2
0.9843	23.46	1.173	0.1699	-2.705	3.495	22.14	22.61	- 3.6
3.937	5.902	1.182	0.1546	-0.6189	0.9412	4.742	5.687	- 3.6
19.69	1.459	1.212	0.1035	-0.0985	0.3173	0.3442	1.443	- 1.1
49.21	1.068	1.238	0.0592	-0.0264	0.3070	-0.0154	1.066	- 0.1
98.43	1.032	1.251	0.0353	-0.0095	0.3260	-0.0369	1.033	+ 0.03
147.6	1.034	1.257	0.0268	-0.0051	0.3349	-0.0321	1.033	- 0.1
196.9	1.037	1.260	0.0217	-0.0035	0.3393	-0.0273	1.037	- 0.05

$* \ Error = \left(C_{Ic-th} - C_I\right)/C_I \times 100$

The differences between C_{I-th} and C_I at high Reynolds numbers are basically related to the shape of the mean velocity profile and its deformation in the vicinity of the sudden expansion. For a highly shear-thinning fluid the mean velocity approaches a plug shape and the distortions in this shape are more difficult to happen for two reasons: first, the distortions in the upstream velocity profile on approaching the expansion are in order to flatten the profile. Since the profiles are already flatter due to shear-thinning, smaller changes take place. Secondly, the flatter velocity profiles are coupled with higher viscosities in the core of the pipe flow, which makes it more resistant to distortions in the velocity and pressure profiles. Hence, as shear-thinning increases the modifications of the velocity profile become more localised and tend to occur nearer to the wall. This is well shown in Fig. (6) where the momentum shape factor at the end of the inlet pipe (β_{01}) is plotted as a function of the generalised Reynolds number and n. In all cases β_{01} is constant at low Re, then it increases with Re tending to an asymptote at large Re. As n decreases, the values of β_{01} are reduced due to flatter velocity profiles, the rise in β_{01} is delayed to higher Reynolds numbers and the differences between the high and low Reynolds number asymptotes decrease, thus showing a smaller amount of distortion in the upstream velocity profile.

The tables also show well that the most important corrections, ΔC_{F2} (wall friction in outlet pipe) and ΔC_{p0} (non-uniform pressure), increase with shear-thinning at low Reynolds numbers. In contrast, ΔC_{F1} (wall friction in inlet pipe) looks fairly independent of n, except for the lowest n. Of the large corrections ΔC_{p0} is the most important, especially at low Reynolds numbers, and grows in importance as n decreases. This is shown in Fig. (7), where the local loss

coefficient from the flow simulations, C_I, is compared with corrected-theoretical values (C_{Ic-th}) obtained from Eq. (8) with and without taking into account non-uniformity of pressure fields (ΔC_{p0}). Two values of power law index are considered, $n= 0.8$ (mild shear-thinning, Fig. (7-a)) and $n= 0.4$ (strong shear-thinning, Fig. (7-b)). Clearly, pressure non-uniformity has an important contribution at low Reynolds numbers, in particular at low n, Fig. (7-b). By neglecting its effect, i.e. by assuming a uniform pressure, the predictions of the corrected-theory show the opposite trend to that of the variation of C_I with Re_{gen}.
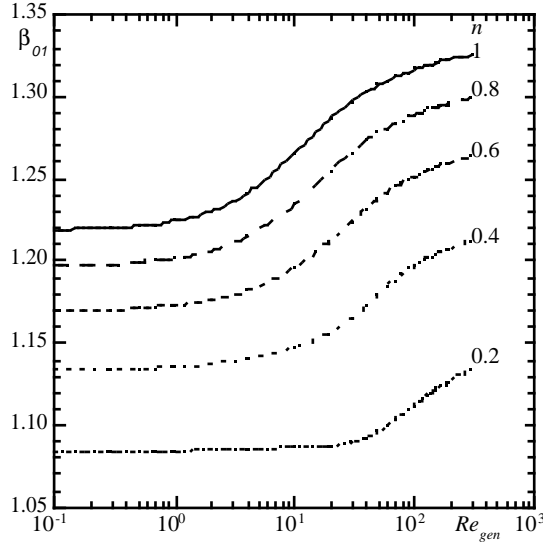

Figure 6. Variation of the momentum shape factor at the end of the inlet pipe with Reynolds number and power index of power law fluids in a 1:2.6 expansion.
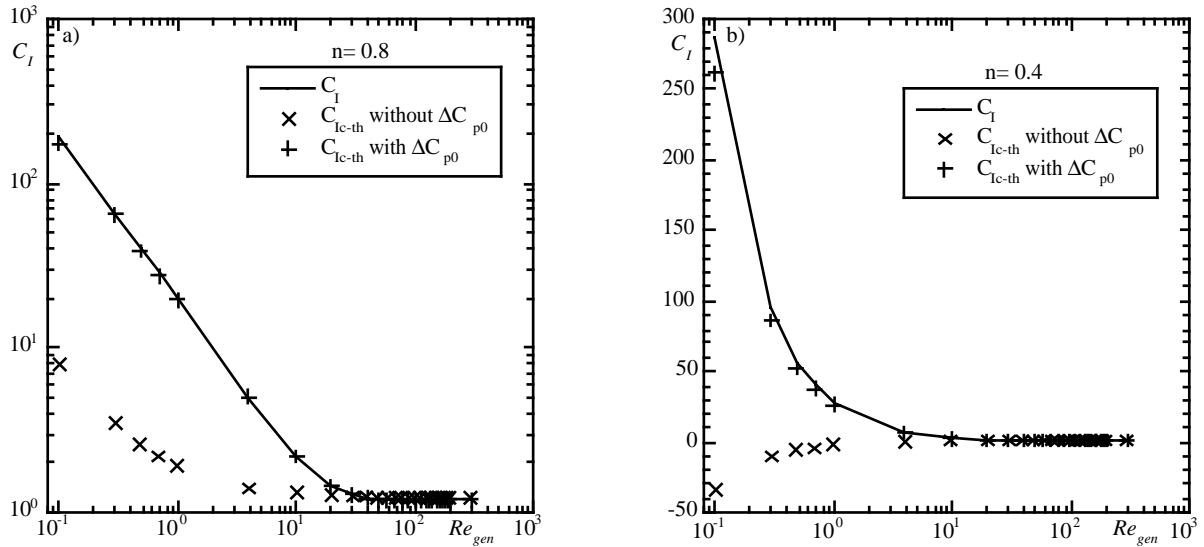

Figure 7. Effect of n on the pressure correction ΔC_{p0} to C_I: a) $n = 0.8$, b) $n= 0.4$.

4.4. Engineering correlation for C_I

More useful from an engineering point of view is a correlation for the local loss coefficient as a function of Re_{gen} and n. Following our previous work for Newtonian fluids (Oliveira et al, 1998), the following correlation, obtained by best-fitting techniques, is proposed

$$C_I = \frac{m_1}{Re_{gen}^{m_2}} + m_3 + m_4 \times \log(Re_{gen}) + m_5 \times \log^2(Re_{gen}) \qquad (12)$$

where the m_i coefficients are given by the expressions:

$$m_1 = 17.45 - 27.53 \times \log(n)$$

$$m_2 = 1 - 0.009n + 0.0027n^2 - 0.010n^3$$

$$m_3 = 0.113 - 1.02n$$

$$m_4 = -0.256 + 1.21n + 0.498n^2$$

$$m_5 = 0.124 - 0.0911n - 0.149n^2 - 0.110n^3 \tag{13}$$

These expressions are to be used only for a sudden axisymmetric expansion with a diameter ratio of 1: 2.6 in the range of $0.2 \leq n \leq 1$ and $0.09 \leq Re_{gen} \leq 200$. Expression (12) gives computed values of C_I with accuracies better than 3% at low and high Reynolds numbers and of about 5-6% at intermediate Reynolds numbers.

5. Conclusions

A numerical investigation was carried out to obtain the variation of the local loss coefficient C_I through a 1:2.6 sudden expansion for power law fluids. The effects of shear-thinning and Reynolds number were assessed. The variation of the recirculation length and of the eddy strength were also quantified. The main findings were:
- the normalized recirculation length decreased with shear-thinning, and in all cases two regions of behaviour were observed: a linear variation of X_R at high Reynolds numbers and an asymptotic behaviour as the Reynolds number tended to zero that also depended on n;
- The eddy strength weakened with shear-thinning and also exhibited an asymptotic value at low Reynolds numbers. However, at high Reynolds numbers its variation with Re was not linear;
- At low Reynolds numbers the flow was viscous-dominated and the local loss coefficient varies inversely with the Reynolds number. When Re_{gen} was employed, the loss coefficient was found to increase with shear-thinning by more than 100% when n decreased from 1 to 0.2;
- At high generalised Reynolds numbers, C_I tended to a constant value which decreased with shear-thinning. When employing Re_{gen} a variation in excess of 50% was found when n decreased from 1.0 to 0.2;
- Contrasting with the two previous points, it was found that C_I always decreased monotonically with decreasing n, if the modified Reynolds number definition was adopted as independent parameter instead of the generalised Reynolds number;
- A correlation was derived for the local loss coefficient, in terms of Re_{gen} and n, to facilitate engineering calculations of pressure losses in piping systems.

6. Acknowledgements

7. References

Back, L. and Roshke, E. 1972. Shear layer regimes and wave instabilities and reattachment lengths downstream of an abrupt circular channel expansion. *J. Applied Mech.*, Sept., 677.

Badekas, D. and Knight, D. D. 1992. Eddy correlations for laminar axisymmetric sudden expansion flows. *ASME J. Fluids Eng.*, vol. 114, pp. 119-121.

Baloch, A., Townsend, P. and Webster, M. F. 1995. On two- and three-dimensional expansion flows. *Computers and Fluids*, vol. 24, pp. 863-882.

Baloch, A., Townsend, P. and Webster, M. F. 1996. On vortex development in viscoelastic expansion and contraction flows. *J. Non-Newt. Fluid Mech.*, vol. 65, pp. 133-149.

Castro, O. S. and Pinho, F. T. 1995. Turbulent Expansion Flow of Low Molecular Weight Shear- Thinning Solutions.*Experiments in Fluids*, vol. 20,pp. 42-55.

Coates, P. J., Armstrong, R. C. and Brown, R. A. 1992. Calculation of steady-state viscoelastic flow through axisymmetric contractions with the EEME formulation. *J. Non-Newt. Fluid Mech.*, vol. 42, pp. 141-188.

Edwards, M. F., Jadallah, M. S. M. and Smith, R. 1985. Head losses in pipe fittings at low Reynolds numbers. *Chem. Eng. Res. Des.*, vol. 63, pp. 43-50.

Escudier, M.P. and Smith, S. 1999. Turbulent flow of Newtonian and shear-thinning liquids through a sudden axisymmetric expansion. *Exp. in Fluids*, vol. 27, pp. 427-434.

Ferziger, J. H. 1981. Numerical methods for engineering applications. John Wiley & Sons, Inc.

Gupta, R. C. 1965. Expansion losses in laminar flows of non-Newtonian fluids. *Bulletin of the Calcutta Mathematical Society*, vol. 57, pp. 117-122.

Habib, M. A. and Whitelaw, J. H. 1982. The calculation of turbulent flow in wide-angle diffusers. *Num. Heat Trans.*, vol. 5, pp. 145

Halmos, A. L., Boger, D. V. and Cabelli, A. 1975. The behaviour of a power law fluid flowing through a sudden expansion. Part I. Numerical solution. *AIChEJ*, vol. 21, pp. 540-549.

Halmos, A. L. and Boger, D. V. 1975. The behaviour of a power law fluid flowing through a sudden expansion. Part II. Experimental verification. *AIChEJ*, vol. 21, pp. 550-553.

Halmos, A. L. and Boger, D. V. 1976. Flow of viscoelastic polymer solutions through an abrupt 2-to-1 expansion. *Trans. Soc. Rheol.*, vol. 20, pp. 253-264.

Issa, R. and Oliveira, P. J. 1994. Numerical prediction of phase separation in two-phase flow through T-junctions. *Computers and Fluids*, vol. 23, pp. 347-372.

Macagno, E. O. and Hung, T. K. 1967. Computation and experimental study of a captive annular eddy. *J. Fluid Mech.*, vol. 28, pp. 43-.

Metzner, A. B. and Reed, J. C. 1955. Flow of Non-Newtonian fluids - correlation of the laminar, transition and turbulent flow regimes. *A. I. Ch. E. J*, vol. 1, pp. 434-440.

Miranda, J. P. 1999. Numerical investigation of laminar flow of shear-thinning fluids in a sudden expansion. MSc Thesis, Universidade do Porto, Portugal (in Portuguese)

Missirlis, K. A., Assimacopoulos, D. and Mitsoulis, E. 1998. A finite volume approach in the simulation of viscoelastic expansion flows. *J. Non-Newt. Fluid Mech.*, vol. 78, pp 91-118.

Monnet, P., Menard, C. and Sigli, D. 1982. Some new aspects to the slow flow of a viscous fluid through an axisymmetric duct expansion or contraction. II- Experimental part. *Appl. Sci. Res.*, vol. 39, pp. 233-248.

Nguyen, H. and Boger, D. V. 1979. The kinematics and stability of die entry flows. *J. Non-Newt. Fluid Mech.*, vol. 5, pp. 353-368.

Oliveira, P. J. 1992. Computer modelling of multidimensional multiphase flow and application to T- junctions. PhD thesis, Imperial College, University of London.

Oliveira, P. J. and Pinho, F. T. 1997. Pressure drop coefficient of laminar Newtonian flow in axisymmetric sudden expansions *Int. J. Heat and Fluid Flow*, vol. 18, pp. 518-529.

Oliveira, P. J., Pinho, F. T. and Schulte, A. 1998. A general correlation for the local loss coefficient in Newtonian axisymmetric sudden expansions. *Int. J. Heat and Fluid Flow*, vol. 19, pp. 655-660.

Pak, B., Cho, Y. I. and Choi, S. U. S. 1990. Separation and reattachment of non-Newtonian fluid flows in a sudden expansion pipe. *J. Non-Newt. Fluid Mech.*, vol. 37, pp. 175-199.

Pak, B., Cho, Y. I. and Choi, S. U. S. 1991. Turbulent hydrodynamic behaviour of a drag-reducing viscoelastic fluid in a sudden expansion pipe. *J. Non-Newt. Fluid Mech.*, vol. 39, pp. 353-373.

Pereira, A. S. and Pinho, F. T. 2000. Turbulent characteristics of shear-thinning fluids in recirculating flows. *Exp. in Fluids* vol. 28, N. 3, pp. 266-278.

Pereira, A. S. and Pinho, F. T. 2002. The effect of the expansion ratio on a turbulent non-Newtonian recirculating flow. *Exp. in Fluids*, vol. 32, pp. 458-471.

Pinho, F. T. 2001. The Finite-Volume Method Applied to Computational Rheology: II-Fundamentals For Stress-Explicit Fluids. *e-rheo.pt*, 1, 63-100 (available at http://www.dep.uminho.pt/e-rheo.pt/)

Scott, P., Mirza, F. and Vlachopoulos, J. 1986. A finite element analysis of laminar flows through planar and asisymmetric abrupt expansions. *Computers and Fluids*, vol. 14, pp. 423-432.

Stieglmeier, M., Tropea, C., Weiser, N. and Nitsche, W. 1989. Experimental investigation of the flow through axisymmetric expansions. *J. Fluids Eng.*, vol. 111, pp. 464-471.

8. Copyright Notice